DESIGN OF A 10 fs ELECTRON BEAM WITH A PHOTOCATHODE RF GUN AND AN RF BUNCHER

Jang-Hui Han, Diamond Light Source, Oxfordshire, United Kingdom.

Abstract

We discuss the possibility to produce an electron beam for a diffraction experiment with a 10 fs resolution. In this design, an S-band photocathode RF gun was used for generating and accelerating a beam and an S-band cavity was used for bunching the beam. Numerical optimization was done for a 6 fs fwhm length and a 40 μrad divergence with a charge of 1.6 pC (10^7 electrons). Beam arrival time jitter at the target was simulated as 11.4 fs when state-of-the-art RF parameters are used.

INTRODUCTION

In a photocathode RF gun, the initial pulse length of an electron beam is controlled with a drive laser pulse. The photoemission response time is far shorter than one femtosecond for a metal cathode [1]. Ultrashort beam generation systems with a RF gun have been built in a few labs for single shot diffraction experiments [2-5]. The electron pulse length is however limited to about 100 fs. When an ultrashort electron beam is launched at the cathode, the space charge force expands the beam. This effect mainly takes place near the cathode where the beam energy is small. To achieve a bunch length below 10 fs a small number of electrons, about 10000 which is insufficient for a single shot experiment, should be used.

Another method to achieve a short bunch is to generate a relatively long bunch at the cathode and compress after the gun where the beam becomes relativistic. The layout of the system is shown in Fig. 1. The gun was designed to operate with a 1 kHz repetition rate [6]. The gun section is identical to the gun for a free electron laser injector [7]. A buncher and another solenoid are placed after the gun.

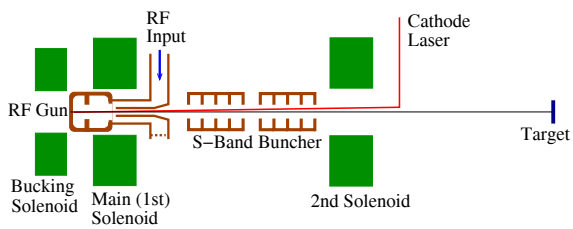

Figure 1: Layout of the system.

When an RF buncher is not used, the accelerating field at the gun should be high enough to minimize the space charge. On the other hand, a strong RF field generates dark current, therefore the RF field strength should not be too high. When an RF buncher is used to compress the bunch length, the gun field does not need to be very high. In this design, the peak gun field is 80 MV/m. The buncher is separated as two cavities to decrease the jitter contribution from the RF phase. As will be discussed later, beam arrival time drift caused by buncher RF phase jitter is more than the bunch length. With two cavities controlled independently, the jitter is reduced by $1/\sqrt{2}$. The 2nd solenoid after the buncher controls the beam divergence and beam size at the target position. This solenoid is the same as the gun main solenoid. Jitter simulation and beam parameter optimization were carried out with ASTRA [8].

BEAM ARRIVAL TIME JITTER

For such a short electron bunch to be useful, the beam arrival time at the target should be stabilized. We use state-of-the-art stability of the RF parameters, 0.013% rms in RF amplitude jitter and 0.014° rms in RF phase jitter, as reported in [9] to simulate arrival time drift.

Since the velocity of a beam after the gun is not fully relativistic, the beam arrival time is sensitive to the change of the gun RF amplitude, i.e. the beam energy. The sensitivity to amplitude jitter depends on the gun phase (Fig. 2). At each gun phase, beam arrival time at 0.45 m, where the buncher starts, was simulated with 9 different gun amplitudes within ±1% variation of 80 MV/m and then a linear fit was made to allow the results to be scaled to the nominal RF amplitude jitter. At gun phases of –20° to 15°, sensitivity to amplitude jitter is not changed. The 0° phase means the phase when the maximum beam energy from the gun is achieved.

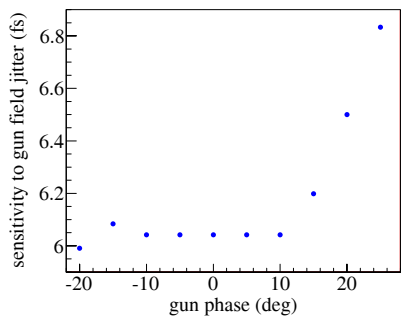

Figure 2: Beam arrival time sensitivity to 0.013% gun RF amplitude jitter.

Beam arrival time dependence on the gun phase (Fig. 3) results from the phase slippage. Up to 15° gun phase, the arrival time gets shorter with a phase increase because the beam experiences a higher RF field when it is emitted from the cathode. However, when the phase increases further the phase slippage gets larger and the beam experiences a deceleration field at the last part of the second cell, where the field direction is reversed before the beam goes out from the gun cavity.

After the gun, the RF buncher rotates the longitudinal beam phase space clockwise for a velocity bunching. When the beam is configured so that the head slice has a low energy, a smaller phase space rotation, by a less RF amplitude or a less RF phase offset from –90°, is

necessary. This means that jitter contribution from the buncher is small. Figure 4 shows the longitudinal phase spaces for various gun phases. With negative phases we can get a preferred beam distribution.

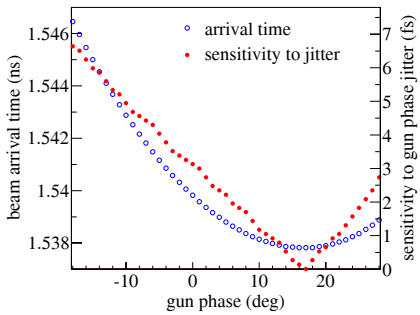

Figure 3: Beam arrival time at 0.45 m depending on gun phase and the sensitivity to 0.014° phase jitter.

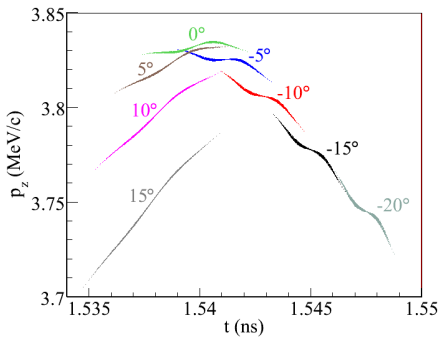

Figure 4: Beam longitudinal phase space for various gun phases at 0.45 m.

Arrival time drift caused by gun phase jitter is partially compensated by the phase of the bunchers. With a gun phase shifted to the positive direction, the beam has higher beam energy and the arrival time at the buncher is sooner. Due to the earlier arrival at the buncher, the beam experiences a buncher phase shifted to the negative direction. The beam then gets more deceleration within the buncher. For the case that a beam starts with a negative gun phase, the opposite is true.

Arrival time drift by gun amplitude jitter is hardly compensated by the buncher because the beam energy difference is too much to be fully compensated.

After considering the effects discussed above and testing with simulation, a gun phase of −15° was chosen to minimize overall arrival time sensitivity. Jitter contribution from buncher amplitude and phase was simulated after finding optimum machine parameters for the best beam performance. In reality, several iterations were made to find the optimum condition for the best beam performance and low arrival time jitter.

BEAM PERFORMANCE

As discussed above, beam parameter optimization was done with solenoid fields and buncher RF amplitude and phase from the previously chosen gun amplitude and phase. The simulation input parameters and the optimized result are summarized in Table 1. The beam energy and rms bunch length evolution is shown in Fig. 5.

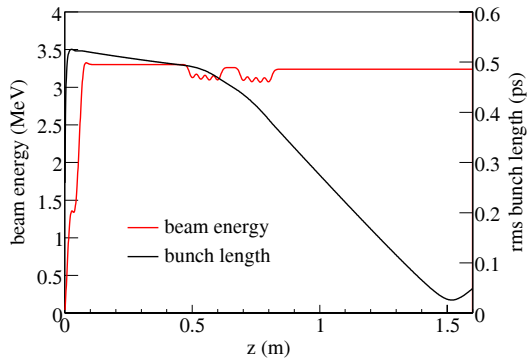

Figure 5: Beam energy and rms bunch length.

Since a beam is launched with negative gun phase from the maximum energy gain phase, the energy of the bunch head has a lower energy than of the tail (Fig. 6a). This energy chirp is increased with the buncher (Fig. 6b) so that the bunch gets compressed. At about 1.5 m, the rms length becomes minimal (Fig. 6c). But, the ultimate peak current is achieved at 1.6 m where the central slices are aligned vertically (Fig. 6d). The peak current is 122 A and the fwhm bunch length is 6 fs (Fig. 7).

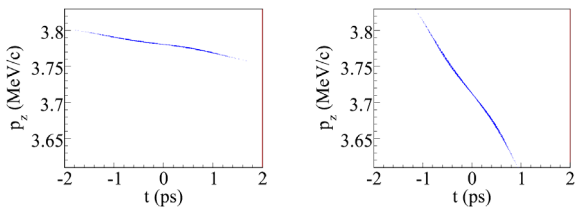

(a) After gun (0.1 m). (b) After buncher (0.85 m).

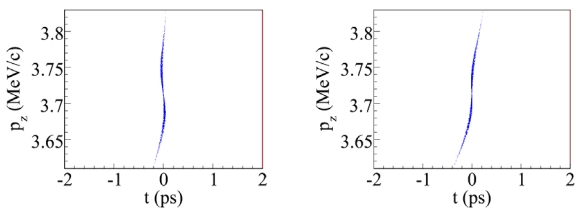

(c) At 1.5 m. (d) At 1.6 m.

Figure 6: Beam longitudinal phase spaces.

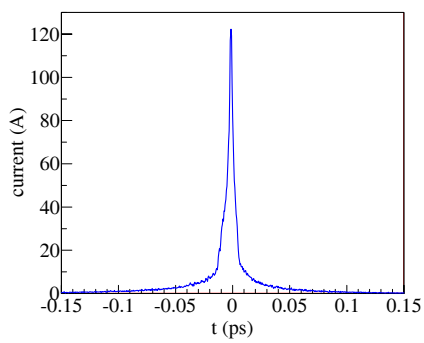

Figure 7: Temporal distribution of a 1.6 pC beam. The peak current is 122 A and the fwhm length is 6 fs.

The beam divergence should be as small as 50 μrad for a MeV beam to be clearly imaged after diffraction with a sample [10]. Here, the rms divergence of a 1.6 pC beam is 40 μrad (Fig. 8). The rms beam size is 0.62 mm.

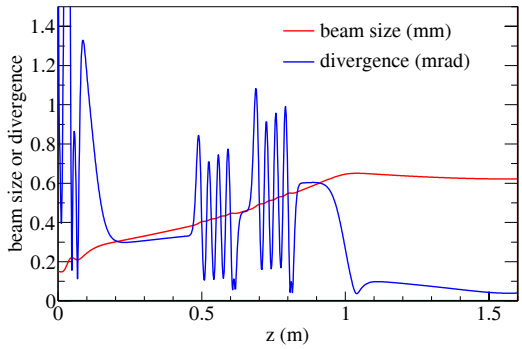

Figure 8: Beam size and divergence in rms.

The slice parameters of the beam transverse emittance and energy spread are shown in Fig. 9. The machine and beam parameters are summarized in Table 1.

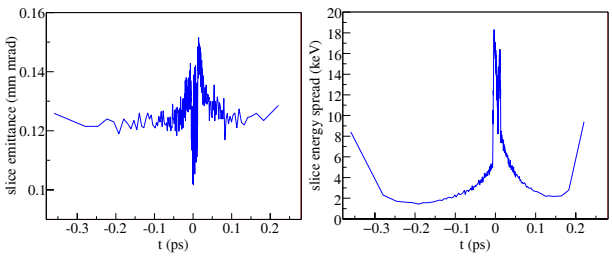

(a) Slice emittance. (b) Slice energy spread.

Figure 9: Temporally sliced beam parameters.

Table 1: Simulation input parameters of laser, gun and bunchers and the simulation results with ASTRA at 1.6 m.

Parameters		Values
Laser	pulse length (rms)	0.9 ps
	radius	0.3 mm
	E_{kin} of emitted e^-	0.6 keV
	thermal ε	0.1211 mm mrad
Gun	peak field at cathode	80 MV/m
	phase from on-crest	–15°
Buncher 1	max field	18 MV/m
	phase from on-crest	–92°
Buncher 2	max field	18 MV/m
	phase from on-crest	–91.6°
Main gun solenoid	position from cathode	0.11 m
	peak field	0.195 T
2nd solenoid	position from cathode	1.0 m
	peak field	0.0878 T
Beam at 1.6 m	number of electrons	10^7
	bunch length (fwhm)	6 fs
	peak current	122 A
	divergence	39.9 μrad
	beam size	0.619 mm
	100% projected ε	0.179 mm mrad
	central slice ε	0.125 mm mrad
	mean E (MeV)	3.24 MeV
	$\Delta E/E$ at center	0.31%

For the condition with the beam focused at the target location (1.6 m) longitudinally and transversely, the various jitter contributions were simulated. Adding all contributions quadratically, the estimated arrival time jitter is 11.4 fs rms (Table 2).

Table 2: Beam arrival time sensitivity to RF jitter.

Error sources		Arrival time jitter in fs
Gun	0.013% field	6.24
	0.014° phase	1.7
Buncher 1	0.013% field	0.2
	0.014° phase	7.1
Buncher 2	0.013% field	0.2
	0.014° phase	6.1
Total		11.4

SUMMARY AND OUTLOOK

With a system consisting of an S-band gun and a buncher, a 6 fs beam at 1.6 pC was simulated. The peak current reaches 122 A. The rms beam divergence and rms beam size at the target are 40 μrad and 0.62 mm. However, rms beam arrival time jitter was 11.4 fs when state-of-the-art RF parameters were used. In order to have a 10 fs resolution, the total beam arrival time jitter should be 8 fs or less. To satisfy such a tolerance, amplitude jitter should be less than 0.01% and phase jitter should be less than 0.01°. More study to increase the system tolerance is required to have a time resolution better than 10 fs.

By using the gun designed for 1 kHz repetition rate at 100 MV/m peak field at the cathode [6], this ultrashort beam generation system which operates at 80 MV/m should be capable of running with a 1.5 kHz repetition rate.

ACKNOWLEDGEMENTS

JHH would like to thank G. Materlik and R. Walker for encouraging this study.

REFERENCES

[1] A. Cavalieri et al., Nature **449**, 1029 (2007).
[2] J. B. Hastings et al., Appl. Phys. Lett. **89**, 184109 (2006).
[3] R. K. Li. et al., Rev. Sci. Instrum. **80**, 083303 (2009).
[4] J. Yang. et al., Rad. Phys. Chem. **78**, 1106 (2009).
[5] P. Musumeci et al., Rev. Sci. Instrum. **81**, 013306 (2010).
[6] J.-H. Han, These Proceedings, THP104.
[7] J.-H. Han, These Proceedings, THP105.
[8] K. Floettmann, A Space Charge Tracking Algorithm (ASTRA), http://www.desy.de/~mpyflo.
[9] T. Asaka et al., IPAC10, p. 2194.
[10] X. J. Wang et al., J. Korean Phys. Soc. **48**, 390 (2006).